

Mis-trafficking of Endosomal Urokinase Proteins Triggers Drug-Induced Glioma Non-Apoptotic Cell Death.

Nagarekha Pasupuleti, Ana Cristina Grodzki and Fredric Gorin

Department of Neurology, School of Medicine (N.P., F.G.) and Department of Molecular Biosciences, School of Veterinary Medicine (N.P., F.G., A.C.G.), University of California, Davis, California

Running Title: UCD38B alters endosomal trafficking in gliomas

Corresponding Authors

1. Fredric Gorin

Professor

Department of Neurology (Med),

Department of Molecular Biosciences (Vet)

University of California, Davis Comprehensive Cancer Center

Phone: [916-734-6284](tel:916-734-6284)

Fax: 916-734-6525

E-mail: fagorin@ucdavis.edu

2. Nagarekha Pasupuleti

Assist. Project Scientist

Department of Neurology (Med),

Department of Molecular Biosciences (Vet)

University of California, Davis Comprehensive Cancer Center

Phone: [530-752-2827](tel:530-752-2827)

E-mail: npasupul@ucdavis.edu

Text pages : 37

Figures : 11

Tables : 1

References : 36

Abstract: 250 words

Introduction: 619 words

Discussion: 1529 words

Abbreviations: HGG, high grade-gliomas; CIC, cancer initiating cells; uPAS, urokinase plasminogen activator system; uPA, urokinase plasminogen activator; PAI-1, plasminogen activator inhibitor-1; uPAR, urokinase plasminogen activator receptor; tPA, tissue plasminogen activator; LRP-1, LDL Receptor-related protein-1; RAP, receptor associated protein; AIF, apoptosis-inducing factor; PARP, poly ADP-ribose polymerase; ECM, extracellular matrix; BSA, bovine serum albumin; mAb, monoclonal antibody; EE, early endosomes; LE, late endosomes.

Abstract

5-benzylglyciny-amiloride (UCD38B) is the parent molecule of a class of anti-cancer small molecules that kill proliferative and non-proliferative high grade glioma cells by programmed necrosis. UCD38B intracellularly triggers endocytosis causing 40-50% of endosomes containing proteins of the urokinase plasminogen activator system (uPAS) to relocate to perinuclear mitochondrial regions. Endosomal 'mis-trafficking' caused by UCD38B in human glioma cells corresponds with mitochondrial depolarization with the release and nuclear translocation of apoptotic inducing factor (AIF) followed by irreversible, caspase-independent cell demise. High content quantification of immunocytochemical co-localization studies identified that UCD38B treatment increased endocytosis of urokinase plasminogen activator (uPA), its receptor uPAR and plasminogen activator inhibitor-1 (PAI-1) into the early and late endosomes by 4 to 5-fold prior to AIF nuclear translocation and subsequent glioma demise. PAI-1 was found to comparably relocate with a subset of early and late endosomes in four different human glioma cell lines after UCD38B treatment, followed by caspase independent, non-apoptotic cell death. Following UCD38B treatment the receptor guidance protein LRP-1, required for endosomal recycling of uPAR to the plasmalemma, remained abnormally associated with PAI-1 in early and late endosomes. The resultant aberrant endosomal recycling increased total cellular content of the uPA- PAI-1 protein complex. Reversible inhibition of cellular endocytosis demonstrated that UCD38B bypasses the plasmalemmal uPAS complex and directly acts intracellularly to alter uPAS endocytotic trafficking. UCD38B represents a class of small molecules whose anti-cancer cytotoxicity is a consequence of causing the mis-trafficking of early and late endosomes containing uPAS cargo and leading to AIF-mediated necrotic cell death.

Introduction

High-grade gliomas (HGGs) are rapidly proliferative, highly infiltrative, and predominantly fatal primary brain cancers with hypovascularized infiltrative borders and characterized by the spontaneous formation of avascular necrotic tumor domains. Within the hypoxic-ischemic regions, HGGs demonstrate increased expression of proteins belonging to the urokinase plasminogen activator system (uPAS) (Harbeck et al., 2013). The major components of the uPA system are urokinase-type plasminogen activator (uPA), tissue-type plasminogen activator (tPA), plasminogen activator inhibitors (PAI-1 and PAI-2), and the uPA receptor (uPAR). uPAS proteins play an important role in events leading to cancer cell infiltration, angiogenesis, and metastasis. uPA is a serine protease synthesized as pro-uPA that is secreted and becomes activated when bound to its cell surface receptor uPAR (Blasi et al., 1987). Activated uPA catalyzes the transformation of plasminogen into plasmin (Ellis et al., 1989). Plasmin is an extracellular serine protease capable of degrading proteins of the extracellular matrix (ECM) and basement membranes (Andreasen et al., 1997). Plasminogen activator inhibitors are anti-proteases belonging to the SERPIN super family that inhibit the enzymatic activities of uPA and tPA. PAI-1 binds to the active site of uPA generating a uPA-PAI-1 protein complex that is bound to the plasmalemmal uPAR receptor (uPAR::uPA-PAI-1). Enzymatic inhibition of secreted and receptor-bound uPA by PAI-1 impedes degradation of the extracellular matrix and fibrinolysis. Despite its enzymatic inhibition of uPA, elevated PAI-1 expression in several cancer cell types, notably high grade glioma and breast cancers, strongly corresponds with enhanced tumor growth, infiltration, angiogenesis, and metastasis (Bajou et al., 2004; Schmitt et al., 1997). Previously, small molecules and antibodies designed to inhibit secreted and plasmalemmal uPA have been investigated as anti-cancer agents but are predominantly cytostatic preventing cancer migration

and angiogenesis (Setyono-Han et al., 2005; Ulisse et al., 2009). These plasmalemmal uPA inhibitors fundamentally differ from the anti-cancer cytotoxicity and the intracellular mechanisms described for 5-benzylglyciny-amiloride (UCD38B) and its peptidomimetic congeners.

The intracellular functions of uPA-PAI-1 are protean and poorly understood. ELISA can quantify protein complexes of uPA-PAI-1, and increased complex expression has been reported to strongly correlate with cancer recurrence and metastasis in lymph node negative breast cancer (Harbeck et al., 2013). A summary of endocytotic trafficking of uPAS proteins is depicted in figure 1. PAI-1 binds to the active site of uPA, the latter bound to its plasmalemmal receptor (uPAR). PAI-1 regulates cancer cell invasion and detachment by controlling endocytic recycling of the uPAR::uPA-PAI-1 complex (Cortese et al., 2008; Czekay et al., 2003). Clathrin-mediated endocytic internalization of this tertiary uPAS complex requires the additional binding by the endocytic guiding receptor protein, LDL receptor-related protein-1 (LRP-1) (Herz et al., 1992; Herz et al., 1988). The resultant quaternary complex is internalized via clathrin-coated pits and transported to early endosomes (EE) and late endosomes (LE) where uPA-PAI-1 becomes dissociated from uPAR. The uPA-PAI-1 complex then undergoes degradation in the lysosomes (Conese et al., 1995; Olson et al., 1992). uPAR and LRP-1 become dissociated and are recycled back from the endosomal compartment to the cell surface (Fig. 1).

Previously, we reported that 5-benzylglyciny-amiloride (UCD38B), a cell permeant, competitive enzymatic inhibitor of uPA, kills proliferating and non-proliferating glioma cells by a novel caspase-independent, programmed necrotic cell death mechanism (Pasupuleti et al., 2013). The current investigation significantly advances these initial observations as we now identify that UCD38B causes AIF-mediated necrotic glioma cell death by re-directing a portion of early and

late endosomes containing uPAS protein cargo with the guiding endosomal LRP-1 receptor protein to perinuclear mitochondrial regions. Surprisingly, we found that cell permeant UCD38B bypasses the plasmalemmal uPAS receptor complex and intracellularly activates endosomal ‘mis-trafficking’. The drug-induced endosomal juxtaposition to the mitochondrial regions temporally corresponds with mitochondrial dilation and depolarization, which is associated with mitochondrial release and nuclear translocation of apoptotic inducing factor (AIF).

Materials and Methods

Drugs and Antibodies

UCD38B (5-benzylglyciny-3-amino-6-chloro-N-(diaminomethylene) pyrazine-2-carboxamide and UCD74A (5-glyciny-3-amino-6-chloro-N-(diaminomethylene) pyrazine-2-carboxamide) were synthesized as described previously (Palandoken et al., 2005; Massey et al., 2012). Drugs stocks of 250 mM were constituted in DMSO stored at -20 °C and reconstituted for each experiment at a final concentration of 250 µM.

Receptor associated protein, (RAP) from Millipore was added to glioma cells at 1 µM for 1 h at 37 °C prior to UCD38B or UCD74A treatment.

Human anti-PAI-1 mouse monoclonal, human anti-LRP-1 goat polyclonal(1:100 dilution; Santa Cruz Biotechnology, Santa Cruz, CA), human anti-EEA-1, human anti-LAMP-1 rabbit polyclonal (1:100 dilution; Abcam, Cambridge, MA) and human anti-uPA mouse monoclonal and human anti- uPAR mouse monoclonal(1:100 dilution; American Diagnostica, Stamford, CT) were used as primary antibodies. Goat anti-mouse secondary antibody (1:20000, Licor Biosciences, Lincoln, NE) was used for protein visualization on immunoblots.

Cell Culture

U87MG, LN229, U118MG and U138MG human glioma cell lines were derived from high grade glial cancers and obtained from the American Type Culture Collection (Manassas, VA). Cells were grown at 37°C and 5% CO₂ in Dulbecco's modified Eagle's medium (Gibco). DMEM or MEM (for U138MG) was supplemented with 10% fetal bovine serum (Hyclone Laboratories,

Rockford, IL), 1% L-glutamine (200 mM, Gibco), 100 U/ml penicillin and 100 mg/ml streptomycin (Gibco, Grand Island, NY).

Cell Death Assay

Lactate dehydrogenase (LDH) assay measured the release of cytosolic LDH from dead and dying glioma cells. Ten thousand cells per well were plated in 96-well microtiter plate and treated with the drugs for 24 h at 37 °C, 5% CO₂. LDH assay was performed according to the manufacturer's protocol (Clontech Laboratories, Mountain View, CA). Absorbance was read at 492 nm using a SpectraMax M3 with SoftmaxPro software (LifeSciSoft, Kingston, NY).

For Trypan blue exclusion assay, cells were harvested by gently rinsing with PBS. Trypan blue was added to cell suspension (10% v/v) and after 3 min an aliquot was transferred to a hemacytometer for manual cell counting.

Immunofluorescence confocal microscopy

Human U87MG glioma cells were cultured in chamber slides. Cells were treated with UCD38B or UCD74A for 30, 60 and 120 min at 250 μM at 37 °C. Mitochondria were visualized by staining with MitoTracker or JC-1 (Molecular Probes, Eugene, OR) for 30 min prior to brief fixation. Cells were washed with PBS and fixed with 4% paraformaldehyde in PBS at room temperature for 15 min, followed by washing with PBS and permeabilized with 80% methanol in PBS at -20 °C for 15 min. Blocking of non-specific antibody binding sites was performed using 3% non-fat dry milk/1% BSA in PBS for 1 h at room temperature. Cells were incubated with primary antibody in 0.1% BSA/PBS at 4 °C, overnight at 1:100 dilution. Secondary antibody against mouse or rabbit, conjugated with Alexa Fluor 488, 594 and 647 (Molecular Probes, Eugene, OR) was used at 1:500 dilution in 0.1% BSA/PBS and incubated for 1 h at room

temperature. After the PBS wash, the slides were mounted with mounting media containing 4', 6-diamidino-2-phenylindole (DAPI; Molecular Probes, Eugene, OR). Images were captured using 40X objective with a spinning disk confocal microscope (Olympus IX81). UCD38B and UCD74A are comparable in quantum yield when visualized by fluorescent microscopy as previously described (Palandoken et al., 2005).

Quantification of co-localized, immunocytological fluorescent biomarkers

Quantification of double labeled immunocytological markers that were co-localized was performed by imaging and analyzing cells using an automated high content imaging system, ImageXpress Micro XL System (Molecular Devices, Sunnyvale, CA, USA). High content imaging was performed on 4 wells per treatment, with 36 sites per well, using a Custom Module, software of MetaXpress 5.0 developed specifically for cytological co-localization studies. A minimum of 10 cells per site was included and sites without cells were excluded when calculating the mean and standard deviation analysis.

Electron Microscopy

U87MG glioma cells were plated in Lab-Tek® Permanox chamber 8-well slides from Electron Microscopy Sciences, Hatfield, PA. Cells were treated with drugs UCD38B, UCD74A or vehicle control at 250 μ M for 1 h. Cells were fixed in Karnovsky's fixative (2.5% glutaraldehyde and 2.0% paraformaldehyde) for 1 h. Slides were prepared as described previously (Pasupuleti et al., 2013). Cells were imaged in the Philips 120 BioTwin electron microscope at 80KV equipped with a Gatan MegaScan, model 794/20 digital camera.

Protein fractionation and immunoblotting

Protein extracts were made in RIPA lysis buffer (Cell Signaling, Danvers, MA) and 50 µg of protein was loaded on SDS-PAGE. For mitochondrial enriched fractions, cells were harvested, washed with 1X PBS and centrifuged 1000 rpm for 5 min. Cells were then resuspended in mitochondrial isolation buffer (250 mM sucrose, 10 mM Tris-HCL pH7.4 and 0.1 mM EGTA) and homogenized using Dounce homogenizer. Samples were centrifuged at 1000 rpm for 10 min to pellet the nuclei. Supernatant was collected in a new tube and centrifuged at 15, 000 rpm for 20 min to collect the pellet (mitochondrial enriched) and supernatant (cytosol enriched) fractions. The pellet was solubilized in lysis buffer and centrifuged to pellet the debris. Protein samples were size-fractionated through 12% SDS-PAGE and transferred onto nitrocellulose membrane by immunoblotting. Blocking buffer (Licor Biosciences, Lincoln, NE) diluted 1:1 in 1X PBS was used for 1 h at room temperature to prevent non-specific binding sites. Primary antibody incubation was performed overnight at 4 °C. The secondary antibody incubation was carried out at room temperature for 1 h. Goat anti-mouse, goat anti-rabbit and donkey anti-goat secondary antibodies from Licor Biosciences were used at 1:10000 dilution. Bands were visualized and quantified using Odyssey Infrared Imager (Licor Biosciences, Lincoln, NE).

uPA and PAI-1 complex ELISA

The human uPA-PAI-1 protein ELISA assay kit was purchased from Molecular Innovations (Novi MI, USA) with human uPA-PAI-1 complex provided in lyophilized form for standardization. It was reconstituted in 3% BSA/TBS for a final concentration 200 ng/ml. The uPA-PAI-1 complex standard was prepared by serial dilution to obtain 0-100 ng/ml range, and a linear standard curve was generated following the manufacturer instructions. U87MG cells were

treated with UCD38B or UCD74A at 250 μ M for 45 min, 1 h or 2 h. DMSO (0.1% v/v) was used as vehicle. Protein extracts were made and protein concentration was determined by BCA assay. A 96-well plate pre-coated with uPA antibody was provided in the kit. The standard and protein were added to the 96-well plate. The plate was incubated at room temperature on a shaker for 30 min. The samples were aspirated and washed with washing buffer included in the kit. Polyclonal PAI-1 antibody was added and incubated again at room temperature for 30 min on a shaker. HRP- linked secondary antibody was added to the wells following the wash. Substrate solution from the kit was added to the wells after the wash and incubated for 5 min. The reaction was stopped by adding 1N H₂SO₄, the plate was gently agitated, and the absorbance was read at 450 nm using a SpectraMax M3 with SoftmaxPro software (LifeSciSoft, Kingston, NY).

Statistical Analysis

Data are presented as mean \pm standard deviation and statistical significance identified using one-way analysis of variance and Bonferroni's nonparametric, multiple pairwise comparisons using SigmaStat software version 2.00 (SPSS Science Inc, Chicago, IL).

Results

UCD38B initiates intracellular relocation of uPA, PAI-1 and uPAR to mitochondrial regions in U87MG glioma cells.

Previously, we determined that cell permeant UCD38B, a competitive enzymatic inhibitor of uPA, after 120 min caused relocation of a portion of intracellular uPA to a mitochondrial enriched subcellular fraction (Pasupuleti et al., 2013). Immunocytochemistry (ICC) localized this uPA migration to perinuclear mitochondrial regions using confocal microscopy (Pasupuleti et al., 2013). PAI-1 binds to the active site of uPA that is bound to uPAR forming plasmalemmal and intracellular uPAR::uPA-PAI-1 complexes. Therefore, we investigated the intracellular localization of PAI-1 and uPAR in U87MG glioma cells following 120 min treatment with UCD38B or its cell impermeant homolog UCD74A. Mitochondria were visualized using MitoTracker and nuclei were stained with DAPI to localize the intracellular distribution of PAI-1 and uPAR following treatment. PAI-1 was distributed homogeneously in the cytoplasm and in the plasmalemmal regions of untreated cells. Following 120 min treatment of UCD38B, a portion of PAI-1 and uPAR were localized to perinuclear mitochondrial regions (Fig. 2A and 3A). In contrast, no alteration in intracellular PAI-1 or uPAR localization was identified following treatment with UCD74A. For biochemical verification, cytosolic and mitochondrial fractions were separated by subcellular fractionation following glioma treatment for 120 min. Immunoblotting was performed to visualize PAI-1 and uPAR using either an anti- PAI-1 or anti-uPAR monoclonal antibody, respectively. Actin and VDAC represented the cytosolic and mitochondrial fractions, respectively. Relative levels of PAI-1 or uPAR expression in each

fraction were normalized to their respective protein markers. Like uPA, PAI-1 and uPAR were enriched in the mitochondrial fractions when treated with UCD38B (Fig. 2B, C and Fig. 3B, C). As a control, neither PAI-1 nor uPAR were enriched in mitochondrial fractions following incubation with cell impermeant UCD74A.

Electron microscopy reveals an increase in endosomal and lysosomal formation in U87MG glioma cells following UCD38B treatment.

Electron micrographs were obtained following 60 min exposure to UCD38B preceding the mitochondrial depolarization observed in live U87MG glioma cells following UCD38B treatment (Pasupuleti et al., 2013). In vehicle-treated control cells, cellular morphology remained unchanged (Fig. 4A). By contrast, U87MG glioma cells treated with UCD38B demonstrated an increase in the formation of endosomes and lysosomes coinciding with the appearance intracellular vacuolization (Fig. 4B). In glioma cells treated with UCD38B, electron microscopy demonstrated that endosomes and lysosomes lay in close proximity to dilated mitochondria with deformed cristae (Fig. 4C). These morphological observations indicated that UCD38B treatment increased endocytosis with an augmentation of endosomes and lysosomes lying in close proximity to dilated mitochondria.

PAI-1 relocation to early and late endosomes is increased following UCD38B treatment in U87MG glioma cells.

Electron microscopy demonstrated that UCD38B treatment within 60 min initiated a marked increase in endocytosis associated with endosomal relocation to mitochondrial regions.

Therefore, we investigated the effect of UCD38B on endosomal trafficking of uPA, PAI-1, and uPAR in U87MG glioma cells. Co-localization of uPAS proteins with early and late endosomes was determined by immunofluorescence confocal microscopy. EEA-1 and LAMP-1 antibodies were used to identify early and late endosomal proteins, respectively. U87MG glioma cells were treated with drug vehicle or UCD74A for 60 min or UCD38B for 15 min and 60 min. PAI-1 did not demonstrate significant co-localization with early or late endosomes following 15 min exposure with UCD38B. However, after 60 min, PAI-1 immunostaining was found to co-localize with endosomes labeled with either EEA-1 or LAMP-1 antibodies (Fig. 5B, and D). No alteration of intracellular PAI-1 colocalization with early or late endosomes was observed in glioma cells following 60 min exposure to either drug vehicle or UCD74A (Fig. 5A and C). U87MG glioma cells were reimaged using the ImageXpress high content imaging system to quantify intracellular co-localization. Following UCD38B treatment for 60 min, PAI-1 co-localized with 40% and 54% of EEA-1 and LAMP-1 immunofluorescent markers for early and late endosomes, respectively. This magnitude of endosomal co-localization of PAI-1 in UCD38B treated cells was highly significant when compared to vehicle- or UCD74A- treated U87MG glioma cells (Fig. 5E).

uPA and uPAR relocation to early and late endosomes is increased following UCD38B treatment in U87MG glioma cells.

Analogously, uPA and uPAR were separately shown to co-localize with EEA-1 and LAMP-1 in glioma cells treated with UCD38B after 60 min but not at 15 min. (Fig. 6B, D and Fig. 7B, 7D). Treatment for 60 min with UCD74A or drug vehicle did not alter the minimal co-localization of uPA and uPAR with EEA-1 and LAMP-1 (Fig. 6A, C and Fig. 7A, C). High content image

analysis quantified that uPA co-localized with early and late endosomal markers 48% and 38 %, respectively in U87MG glioma cells following 60 min treatment with UCD38B (Fig. 6E). Similarly, uPAR co-localized with 49% and 50% of early and late endosomes during this treatment interval (Fig. 7E). Co-localization of uPA and uPAR with early and late endosomes was significant in comparison to vehicle- and UCD74A- treated U87MG glioma cells (Fig. 6E and 7E). After 60 min UCD38B induced a comparable, 4 to 5-fold increase co-localization of PAI-1, uPA, and uPAR with early and late endosomes (Fig. 6E, 7E) that indicated a concerted mechanism of intracellular trafficking.

PAI-1 relocation to early and late endosomes is increased following UCD38B treatment in three additional human glioma cell lines.

Drug-induced relocation of uPAS endosomes as a mechanism leading to AIF-mediated cancer cell necrosis has not previously been described. Therefore, it was important to determine whether endosomal relocation initiated by UCD38B was generalized to additional human glioblastoma cell lines. Because of its regulatory centrality in uPAS endosomal trafficking, PAI-1 was selected as the representative protein to investigate drug-induced endosomal co-localization in the human glioma cell lines LN229, U118MG and U138MG. After 60 min of UCD38B treatment, confocal microscopy and high content imaging again demonstrated that 3 to 5-fold more PAI-1 was co-localized with early and late endosomes in treated LN229 (Supplemental figure 1), U118MG (Supplemental figure 2) and U138MG (Supplemental figure 3) human glioma cells than in vehicle- or UCD74A- treated glioma cells.

LRP-1 and PAI-1 demonstrate a marked increase in relocation to early and late endosomes relocated to mitochondrial regions following UCD38B treatment in U87MG gliomas.

LRP-1 is responsible for guiding clathrin-dependent internalization of the uPA-PAI-1 complex bound to transmembrane uPAR (Fig. 1). Therefore, it was important to identify whether uPAS endocytosis and endosomal trafficking guided by LRP-1 was altered by UCD38B treatment. Confocal microscopy demonstrated that LRP-1 remained abnormally co-localized with intracellular PAI-1 in U87MG glioma cells following 60 min treatment with UCD38B, while no alteration was observed with UCD74A treatment (Fig. 8A). LRP-1 also remained abnormally co-localized with both EEA-1 (Fig. 8B) and LAMP-1 (Fig. 8C) in U87MG glioma cells treated with UCD38B. In glioma cell controls, treated with vehicle or UCD74A, there was no change in LRP-1 localization.

We have used JC-1 in live U87MG glioma cells and determined that mitochondrial depolarization occurred between 60 and 120 min following UCD38B treatment (Pasupuleti et al., 2013). Here, MitoTracker was employed to visualize mitochondria and confocal fluorescent microscopy identified that 60 min treatment of UCD38B caused early (Fig. 9A) and late (Fig. 9B) endosomes to become in close proximity with mitochondria, as compared with glioma cells treated with vehicle or UCD74A. ImageXpress high content quantification demonstrated a 3.5-fold increase in endosomal co-registration with mitochondria (Fig. 9C). To verify that mitochondrial membrane depolarization was associated with this drug-induced co-localization of endosomes with mitochondria, we pre-treated the glioma cells with JC-1 dye. JC-1 forms red aggregates and green monomers in cells having normally polarized mitochondria. The red aggregates are diminished or disappear with mitochondria depolarization or permeabilization.

The late endosomal marker protein LAMP-1 (stained in blue) was selected as a marker of endosomal co-localization within the same glioma cells that had been pre-loaded with JC-1 (Fig 9D). UCD38B treatment for 75 min in glioma cells caused the disappearance JC-1 red aggregates with only the retention of green monomers, indicating mitochondrial depolarization that had increased co-localization with late endosomes (blue) (Fig. 9D). In summary, these data indicated that UCD38B initiated re-trafficking of early and late endosomes containing uPAS and LRP-1 proteins to mitochondria regions and associated with mitochondrial membrane depolarization, which was not observed in glioma cells treated with vehicle or UCD74A.

UCD38B targets intracellular uPAS in U87MG glioma cells rather than plasmalemmal complex.

We then investigated whether the UCD38B targeted the uPA-PAI-1-uPAR complex bound to LRP-1 on plasmalemma. LRP-1 mediated endocytosis was prevented using LRP-1 inhibitor, receptor associated protein (RAP), but did not prevent UCD38B induced glioma cell death as measured by the LDH assay (data not shown). Endosomal trafficking can be reversibly inhibited by cooling glioma cells to 4 °C and then restoring their temperature to 37°C. U87MG glioma cells were exposed to UCD38B or UCD74A at 4 °C for 2, 6 and 24 h, and did not undergo cell death when compared with time-matched controls at 37°C. UCD38B is autofluorescent and can be demonstrated to be intracellular using fluorescent microscopy of washed U87MG cells as we previously described in contrast to autofluorescent cell impermeant UC74A (Leon et al., 2013) (Table 1). UCD38B was observed to be intracellularly localized at 4 °C after a 2 h exposure (Fig. 10 A). We then determined that internalized UCD38B that had entered the glioma cells could initiate endosomal mis-trafficking and subsequent cell death by washing the cells twice at 4 °C

and then shifting them to 37 °C. Glioma cells were incubated at 4 °C for 2 h, 6 h and 24 h. When these glioma cells were shifted to 37 °C for 24 h, intracellular UCD38B killed 40%, 60% and 65% glioma cells, respectively as determined by LDH assay (Fig. 10B) and verified by the trypan blue exclusion assay (Supplemental figure 4). We verified that intracellular UCD38B caused PAI-1 relocation to mitochondrial regions only in glioma cells shifted to 37 °C that subsequently died (Fig. 10C). Importantly, no cell death was detected in control glioma cells under the same conditions when treated with the cell impermeant, autofluorescent congener, UCD74A. Together, these data indicate that UCD38B bypasses the uPAS protein complex in the plasmalemma and directly targets intracellular uPAS proteins to initiate uPAS endosomal relocation that was followed by subsequent glioma cell demise.

uPA-PAI-1 complexes are increased in U87MG glioma cells following treatment with UCD38B treatment.

We postulated that UCD38B was disrupting normal endosomal transport of the quaternary protein complex comprised of uPAR, uPA, PAI-1, and LRP-1. Disruption of uPAS recycling by UCD38B would hamper recycling and the degradation of the quaternary uPAS complex causing an increase in the cellular content of uPA-PAI-1 complexes. A commercially available ELISA kit was employed to quantitatively measure the amount of uPA-PAI-1 complexes in treated and control glioma cells. U87MG glioma cells were treated for 120 min with UCD38B, UCD74A, or drug vehicle. The amount of uPA-PAI complex (in ng/ml) was quantified in 0.5 mg/ml of total protein extracted from the treated glioma cells and normalized to a standard curve (Table 1). Intracellular levels of the uPA-PAI-1 complex were increased significantly following treatment with UCD38B, but not with UCD74A or vehicle control.

Discussion

High grade glial cancers (HGGs), especially WHO grade 4 glioblastomas, are highly aggressive primary cancers of the central nervous system (CNS) accounting for 78% of adult onset primary CNS malignancies (Buckner et al., 2007; Dunn and Black, 2003). The five year survival for patients with glioblastoma multiforme receiving conventional therapy is approximately 9%. Malignant gliomas recur in greater than 90% of cases despite radiation therapy, chemotherapy or anti-angiogenic agents, most notably bevacizumab.

5-benzylglyciny-amiloride (UCD38B) is the parent molecule of a class of anti-cancer small molecules found to kill proliferative and non-proliferative glioma and breast cancer cell types (Leon et al., 2013; Pasupuleti et al., 2013). Previously, we demonstrated that UCD38B is a cell permeant molecule that rapidly initiates a set of intracellular events causing mitochondrial depolarization with the release and nuclear translocation of AIF. Nuclear AIF mediates irreversible programmed necrotic cancer cell death, independent of caspase and PARP activation (Leon et al., 2013; Pasupuleti et al., 2013). The cell impermeant, congener of UCD38B, 5-glyciny-amiloride (UCD74A), is a comparably competitive uPA inhibitor, inhibits cancer cell migration, and is cytostatic but not cytotoxic (Table 1) (Massey et al., 2012; Pasupuleti et al., 2013). Our initial reports describing the anti-cancer cytotoxicity of UCD38B against proliferating and non-proliferating well characterized human glioblastoma and human breast cancer cell lines produced several unanswered questions about its cellular mechanisms that are better understood as a consequence of this investigation.

One important question was why the anti-cancer cytotoxicity of UCD38B is independent of cell cycle. Previously we identified that UCD38B initiates relocation of uPA, and in this study we

identified that uPA along with PAI-1, uPAR, and LRP-1, are coordinately relocated to mitochondrial regions by a concerted drug-induced mis-trafficking of uPAS endosomes. uPA, PAI-1, and uPAR co-localization with early and late endosomes is increased following UCD38B exposure, and corroborated by subcellular fractionation, immunocytochemistry, and quantified by high content cytological image analysis. Co-localization of uPAS proteins with early and late endosomes is increased 4- to 5-fold and approximately 40 to 50% of uPAS endosomes are relocated to perinuclear mitochondrial domains. This unusual anti-cancer drug mechanism of action has not been previously reported so it was important that these observations were generalized to the additional human glioma cell lines LN229, U118MG and U138MG (Supplemental figures 1, 2 and 3). PAI-1 was selected as a representative uPAS protein and demonstrated to co-localize with early and late endosomal markers following treatment with UCD38B. UCD38B initiates intracellular relocation of a subset of uPAS endosomes to perinuclear mitochondrial regions beginning at 60 min of UCD38B treatment which coincides with mitochondrial depolarization in live U87MG glioma cells loaded with the fluorescent dye JC-1 that we previously reported (Pasupuleti et al., 2013). Mitochondrial depolarization is associated with the release and nuclear translocation of AIF triggering a caspase-independent necrotic glioma cell death. This programmed AIF-mediated, caspase-independent glioma cell necrosis following UCD38B treatment is consistently observed in the additional human glioblastoma cell lines LN229, U118MG and U138MG (Supplemental figure 5 and 6) capable of initiating high grade glial tumors.

Endosomal relocation to adjacent mitochondrial domains is triggered by UCD38B within 60 to 120 min corresponding with electron microscopic findings. Electron microscopy showed that UCD38B caused a marked increase in the appearance of vesicles and lysosomes in U87MG

glioma cells following 60 min treatment with UCD38B; consistent with enhanced endocytosis. Confocal microscopy and quantitative image analysis confirmed that UCD38B initiates a 3.5-fold increase in early and late endosomes co-localizing with mitochondrial regions and that 35% of endosomes appear to be relocated following drug treatment. Similar trafficking between endosomes and mitochondria has been reported following cell death caused by VacA toxin produced by *Helicobacter pylori* (Calore et al., 2010), TNF- α (Garcia-Ruiz et al., 2002) and Fas (Ouasti et al., 2007).

AIF-mediated glioma necrosis produced by UCD38B is independent of canonical apoptosis (Pasupuleti 2013, Leon 2013) and appears to be distinct from ripoptosome-mediated necroptosis (Feoktistova et al., 2012). RIP-1 inhibition by necrostatin does not alter the anti-cancer cytotoxicity of UCD38B (Leon et al., 2013). Cell death induced by UCD38B was also unaffected by autophagic inhibition by the AMPK inhibitor compound C, the lysosomotropic agent chloroquine (Meley et al., 2006; Shintani and Klionsky, 2004), or by knockdown of the autophagy protein beclin-1 (Leon et al., 2013). The precise cause of mitochondria membrane depolarization associated with uPAS endosomal co-location initiated by UCD38B remains unclear. Mitochondrial membrane depolarization under these conditions can be triggered by different physiological effectors including calcium-induced calcium release (CICR), reduced concentrations of adenine nucleotides, inorganic phosphate, reactive oxygen species, changes in pH, reduced mitochondrial polarization (Crompton, 1999), and Bax (Marzo et al., 1998). Previously, we reported that calcium overload in glioma cells resulting from reversal of the sodium-calcium exchanger coupled to altered activation of sodium-proton exchange causes increased cytosolic free calcium to be stored within the mitochondria and endoplasmic reticulum (Harley et al., 2010). Calcium signaling released from the endoplasmic reticulum (ER) that are

contacting mitochondrial domains has been described to affect the mode and extent of mitochondrial permeability induced by Bcl proteins (Mattson et al., 2000). The role of mitochondria in participating in programmed necrosis and necroptosis (Marshall and Baines, 2014) and the potential importance of these new cell death mechanisms caused by anti-cancer agents including UCD38B has recently been reviewed and is an active area of cell biological investigation (Fulda, 2013).

LRP-1 is an endosomal guidance protein required for clathrin-mediated endocytosis and uPAS recycling (Cortese et al., 2008). Endocytotic internalization of uPAR bound to uPA-PAI-1 that is mediated by LRP-1 can be prevented by pre-incubating with the specific LRP-1 antagonist receptor associated protein (RAP) (Taylor and Hooper, 2007). UCD38B anti-glioma cytotoxicity was unaffected by pre-incubation with RAP. This surprising result was explained by reversibly inhibiting endosomal trafficking by cooling glioma cells to 4 °C. Intracellular UCD38B, but not UCD74A, was capable of causing endosomal relocation and subsequent glioma demise when endosomal trafficking was re-established at 37 °C. Reversible inhibition of endosomal trafficking demonstrated that cell permeant UCD38B directly enters cancer cells and kills them by selectively mis-trafficking a subset of endosomes containing uPAS cargo.

Early endosomes are normally routed to the juxtannuclear endocytic recycling compartment (ERC) from where the recycling endosomes originate (Grant and Donaldson, 2009; Maxfield and McGraw, 2004). Recycling endosomes transport uPAR and LRP-1 back to the plasma membrane (Fig. 1). Thus, the observed increase in cellular levels of the uPA-PAI-1 complex 60 min after UCD38B treatment can be explained by drug-induced disruption of uPAS endosomal recycling and trafficking causing reduced clearance of transmembrane uPAR bound to uPA and PAI-1 in

the plasmalemma. There is a basal, small co-localization of LRP-1 with PAI-1 that increases significantly following 60 min treatment with UCD38B and is relocated to early and late endosomes along with PAI-1, uPA and uPAR.

Figure 11 summarizes our proposed model for the cellular mechanisms by which intracellular UCD38B binds to the active site of intracellular uPA causing uPA, PAI-1, uPAR, and LRP-1 to be rapidly endocytosed in early and late endosomes. Following UCD38B treatment, early and late endosomes (Steps 1 and 2 respectively) are relocated to mitochondrial regions and followed by the mitochondrial swelling. This mitochondrial swelling corresponds with previously observed mitochondrial depolarization leading to the release and nuclear translocation of AIF. In the nucleus, AIF causes nuclear condensation and caspase-independent glioma necrosis (Step 3). Under normal conditions, uPAR and LRP-1 are recycled back to the cell membrane via recycling endosomes that are disrupted by UCD38B (Step 4). We posit that disrupting this recycling step by UCD38B is responsible for the increase in uPA-PAI-1 protein complexes. Further analysis and refinement of this proposed drug mechanism should provide important insights into why increased uPA-PAI-1 and PAI-1 expression paradoxically has been shown to correspond with a worsened clinical prognosis in several cancer cell types (Andreasen, 2007).

To our knowledge, this is the first report of a class of anti-cancer, cytotoxic small molecules that enter the cancer cell and initiate mis-trafficking of a subset of early and late endosomes containing uPA, PAI-1 and uPAR to mitochondrial domains and triggering irreversible programmed glioma necrotic cell death. Surprisingly, the effect of UCD38B and its 50-fold more potent congeners bypass the plasmalemmal uPAR complex, but instead acts intracellularly to disrupt uPAS endosomal transport. Earlier, we reported the down-regulation of protein

expression of uPA by siRNA and demonstrated its effect on drug cytotoxicity (Pasupuleti et al., 2013). In another study, we have investigated the down-regulation and overexpression of additional uPAS proteins in glioma cells and utilizing a congener of UCD38B, verified AIF-mediated cell death mechanism (unpublished data) within intracerebral glioma xenografts implanted in immunodeficient mice. Remarkably, these small molecules have demonstrated minimal toxicity in rodents when administered systemically or intracerebrally (Pasupuleti and Gorin- in preparation). In subsequent studies, the properties of UCD38B and its 50-fold more potent congeners are being extended to include patient-derived xenografts established from primary human glioblastoma tumors and maintained in immunodeficient mice.

This unusual drug mechanism of action explains why the anti-glioma cytotoxicity of UCD38B was identified as being independent of cell cycle in human glioma and breast cancer cell lines (Leon et al., 2013; Pasupuleti et al., 2013) and appears to be restricted to cancer cell types having altered uPAS expression; notably uPA and PAI-1.

Acknowledgments

We thank Dr. Pamela J. Lein for generous use of her laboratory sharing her Olympus IX81 confocal microscope and ImageXpress Micro XL System.

Author Contributions

Participated in research design: Pasupuleti, N. and Gorin, F.A.

Conducted experiments: Pasupuleti, N.

Performed data analysis: Pasupuleti, N., Grodzki A.C. and Gorin, F.A.

Contributed to the writing of the manuscript: Pasupuleti, N. and Gorin, F.A.

References

- Andreasen PA (2007) PAI-1 - a potential therapeutic target in cancer. *Current drug targets* **8**:1030-1041.
- Andreasen PA, Kjoller L, Christensen L and Duffy MJ (1997) The urokinase-type plasminogen activator system in cancer metastasis: a review. *International journal of cancer Journal international du cancer* **72**:1-22.
- Bajou K, Maillard C, Jost M, Lijnen RH, Gils A, Declerck P, Carmeliet P, Foidart JM and Noel A (2004) Host-derived plasminogen activator inhibitor-1 (PAI-1) concentration is critical for in vivo tumoral angiogenesis and growth. *Oncogene* **23**:6986-6990.
- Blasi F, Vassalli JD and Dano K (1987) Urokinase-type plasminogen activator: proenzyme, receptor, and inhibitors. *The Journal of cell biology* **104**:801-804.
- Buckner JC, Brown PD, O'Neill BP, Meyer FB, Wetmore CJ and Uhm JH (2007) Central nervous system tumors. *Mayo Clinic proceedings* **82**:1271-1286.
- Calore F, Genisset C, Casellato A, Rossato M, Codolo G, Esposti MD, Scorrano L and de Bernard M (2010) Endosome-mitochondria juxtaposition during apoptosis induced by H. pylori VacA. *Cell death and differentiation* **17**:1707-1716.
- Conese M, Nykjaer A, Petersen CM, Cremona O, Pardi R, Andreasen PA, Gliemann J, Christensen EI and Blasi F (1995) alpha-2 Macroglobulin receptor/Ldl receptor-related protein(Lrp)-dependent internalization of the urokinase receptor. *The Journal of cell biology* **131**:1609-1622.
- Cortese K, Sahores M, Madsen CD, Tacchetti C and Blasi F (2008) Clathrin and LRP-1-independent constitutive endocytosis and recycling of uPAR. *PloS one* **3**:e3730.
- Crompton M (1999) The mitochondrial permeability transition pore and its role in cell death. *The Biochemical journal* **341 (Pt 2)**:233-249.
- Czekay RP, Aertgeerts K, Curriden SA and Loskutoff DJ (2003) Plasminogen activator inhibitor-1 detaches cells from extracellular matrices by inactivating integrins. *J Cell Biol* **160**:781-791.

- Dunn IF and Black PM (2003) The neurosurgeon as local oncologist: cellular and molecular neurosurgery in malignant glioma therapy. *Neurosurgery* **52**:1411-1422; discussion 1422-1414.
- Ellis V, Scully MF and Kakkar VV (1989) Plasminogen activation initiated by single-chain urokinase-type plasminogen activator. Potentiation by U937 monocytes. *The Journal of biological chemistry* **264**:2185-2188.
- Feoktistova M, Geserick P, Panayotova-Dimitrova D and Leverkus M (2012) Pick your poison: the Ripoptosome, a cell death platform regulating apoptosis and necroptosis. *Cell cycle* **11**:460-467.
- Fulda S (2013) The mechanism of necroptosis in normal and cancer cells. *Cancer biology & therapy* **14**:999-1004.
- Garcia-Ruiz C, Colell A, Morales A, Calvo M, Enrich C and Fernandez-Checa JC (2002) Trafficking of ganglioside GD3 to mitochondria by tumor necrosis factor- α . *The Journal of biological chemistry* **277**:36443-36448.
- Grant BD and Donaldson JG (2009) Pathways and mechanisms of endocytic recycling. *Nature reviews Molecular cell biology* **10**:597-608.
- Harbeck N, Schmitt M, Meisner C, Friedel C, Untch M, Schmidt M, Sweep CG, Lisboa BW, Lux MP, Beck T, Hasmuller S, Kiechle M, Janicke F, Thomssen C and Chemo NSG (2013) Ten-year analysis of the prospective multicentre Chemo-N0 trial validates American Society of Clinical Oncology (ASCO)-recommended biomarkers uPA and PAI-1 for therapy decision making in node-negative breast cancer patients. *European journal of cancer* **49**:1825-1835.
- Harley W, Floyd C, Dunn T, Zhang XD, Chen TY, Hegde M, Palandoken H, Nantz MH, Leon L, Carraway KL, 3rd, Lyeth B and Gorin FA (2010) Dual inhibition of sodium-mediated proton and calcium efflux triggers non-apoptotic cell death in malignant gliomas. *Brain research* **1363**:159-169.
- Herz J, Clouthier DE and Hammer RE (1992) LDL receptor-related protein internalizes and degrades uPA-PAI-1 complexes and is essential for embryo implantation. *Cell* **71**:411-421.

Herz J, Hamann U, Rogne S, Myklebost O, Gausepohl H and Stanley KK (1988) Surface location and high affinity for calcium of a 500-kd liver membrane protein closely related to the LDL-receptor suggest a physiological role as lipoprotein receptor. *The EMBO journal* **7**:4119-4127.

Leon LJ, Pasupuleti N, Gorin F and Carraway KL, 3rd (2013) A cell-permeant amiloride derivative induces caspase-independent, AIF-mediated programmed necrotic death of breast cancer cells. *PloS one* **8**:e63038.

Marshall KD and Baines CP (2014) Necroptosis: is there a role for mitochondria? *Frontiers in physiology* **5**:323.

Marzo I, Brenner C, Zamzami N, Jurgensmeier JM, Susin SA, Vieira HL, Prevost MC, Xie Z, Matsuyama S, Reed JC and Kroemer G (1998) Bax and adenine nucleotide translocator cooperate in the mitochondrial control of apoptosis. *Science* **281**:2027-2031.

Massey AP, Harley WR, Pasupuleti N, Gorin FA and Nantz MH (2012) 2-Amidino analogs of glycine-amiloride conjugates: inhibitors of urokinase-type plasminogen activator. *Bioorganic & medicinal chemistry letters* **22**:2635-2639.

Mattson MP, LaFerla FM, Chan SL, Leissring MA, Shepel PN and Geiger JD (2000) Calcium signaling in the ER: its role in neuronal plasticity and neurodegenerative disorders. *Trends in neurosciences* **23**:222-229.

Maxfield FR and McGraw TE (2004) Endocytic recycling. *Nature reviews Molecular cell biology* **5**:121-132.

Meley D, Bauvy C, Houben-Weerts JH, Dubbelhuis PF, Helmond MT, Codogno P and Meijer AJ (2006) AMP-activated protein kinase and the regulation of autophagic proteolysis. *The Journal of biological chemistry* **281**:34870-34879.

- Olson D, Pollanen J, Hoyer-Hansen G, Ronne E, Sakaguchi K, Wun TC, Appella E, Dano K and Blasi F (1992) Internalization of the urokinase-plasminogen activator inhibitor type-1 complex is mediated by the urokinase receptor. *The Journal of biological chemistry* **267**:9129-9133.
- Ouasti S, Matarrese P, Paddon R, Khosravi-Far R, Sorice M, Tinari A, Malorni W and Degli Esposti M (2007) Death receptor ligation triggers membrane scrambling between Golgi and mitochondria. *Cell death and differentiation* **14**:453-461.
- Palandoken H, By K, Hegde M, Harley WR, Gorin FA and Nantz MH (2005) Amiloride peptide conjugates: prodrugs for sodium-proton exchange inhibition. *The Journal of pharmacology and experimental therapeutics* **312**:961-967.
- Pasupuleti N, Leon L, Carraway KL, 3rd and Gorin F (2013) 5-Benzylglyciny-amiloride kills proliferating and nonproliferating malignant glioma cells through caspase-independent necroptosis mediated by apoptosis-inducing factor. *The Journal of pharmacology and experimental therapeutics* **344**:600-615.
- Schmitt M, Harbeck N, Thomssen C, Wilhelm O, Magdolen V, Reuning U, Ulm K, Hofler H, Janicke F and Graeff H (1997) Clinical impact of the plasminogen activation system in tumor invasion and metastasis: prognostic relevance and target for therapy. *Thrombosis and haemostasis* **78**:285-296.
- Setyono-Han B, Sturzebecher J, Schmalix WA, Muehlenweg B, Sieuwerts AM, Timmermans M, Magdolen V, Schmitt M, Klijn JG and Foekens JA (2005) Suppression of rat breast cancer metastasis and reduction of primary tumour growth by the small synthetic urokinase inhibitor WX-UK1. *Thrombosis and haemostasis* **93**:779-786.
- Shintani T and Klionsky DJ (2004) Autophagy in health and disease: a double-edged sword. *Science* **306**:990-995.

Taylor DR and Hooper NM (2007) The low-density lipoprotein receptor-related protein 1 (LRP1)

mediates the endocytosis of the cellular prion protein. *The Biochemical journal* **402**:17-23.

Ulisse S, Baldini E, Sorrenti S and D'Armiento M (2009) The urokinase plasminogen activator system: a

target for anti-cancer therapy. *Current cancer drug targets* **9**:32-71.

Footnotes

This research was funded by National Institutes of Health, Neurological Sciences [Grant NS040489, NS060880] by UC Davis School of Medicine, UC Davis Research Investments in Science and Engineering (RISE) and by the MIND Institute Intellectual and Developmental Disabilities Research Center (IDDRC) [Grant U54 HD079125].

Figure legends

Figure 1. uPAS in glioma cells. uPA binds to plasmalemmal receptor uPAR and converts plasminogen to plasmin for extracellular matrix degradation. PAI-1 binds to the active site of uPA, bound to uPAR to form a uPAR::uPA-PAI-1 complex. Endocytic receptor protein, LRP-1 mediates internalization of the uPAS complex into early endosomes and late endosomes. uPA-PAI-1 is dissociated from uPAR and LRP-1 in late endosomes to undergo degradation in the lysosomes. Dissociated uPAR and LRP-1 are recycled back from the endosomal compartment to the cell surface.

Figure 2. Localization of PAI-1 in U87MG glioma cell. Intracellular localization of PAI-1 was visualized by confocal microscopy with an anti-PAI-1 antibody in U87MG cells that had been treated for 120 min with 250 μ M of UCD38B, UCD74A or vehicle (0.1% v/v DMSO) (A). Alexa 488 was used as secondary antibody. MitoTracker and DAPI were used to visualize the mitochondria and nucleus, respectively, and the scale bar is 50 microns. Cytosolic (C) and mitochondrial (M) enriched fractions were separated by SDS-PAGE. PAI-1 was visualized on an immunoblot with Actin and VDAC as cytosolic and mitochondrial marker proteins, respectively (B). Densitometry of PAI-1 expression, normalized to marker proteins, (C) is presented as the mean \pm S.D. of $n = 3$ with $***P < 0.001$.

Figure 3. Localization of uPAR in U87MG glioma cells. U87MG cells were treated for 120 min with 250 μ M of UCD38B, UCD74A or vehicle (0.1% v/v DMSO) (A). Anti-uPAR antibody was used to detect uPAR by immunofluorescence confocal microscopy. Alexa 488 was used as secondary antibody. MitoTracker and DAPI were used to visualize the mitochondria and nucleus, respectively. Scale bar is 50 microns. uPAR levels in cytosolic (C) and mitochondrial

(M) enriched fractions was detected on immunoblots (B) with Actin and VDAC used as cytosolic and mitochondrial marker proteins, respectively. Normalized protein levels of uPAR in cytosolic and mitochondrial fractions were determined by densitometry (C) as the mean \pm S.D. of $n = 3$ with $***P < 0.001$.

Figure 4. Electron Microscopy reveals endocytosis in U87MG glioma cells. Time-matched, vehicle treated (control) U87MG glioma cells (A). U87MG glioma cells were treated with UCD38B at 250 μ M for 60 min and cellular changes were identified by electron microscopy. Arrows indicate increase in cytoplasmic vacuolization (B) and lysosomes formation in UCD38B treated cells (C). Scale bar is 1 micron.

Figure 5. Co-localization of plasminogen activator type 1 (PAI-1) with early and late endosomes in U87MG glioma cells. Co-localization of PAI-1 with early endosomes (EE) using EEA-1 as an early endosome marker protein was detected by immunofluorescent confocal microscopy. U87MG cells were treated with drug vehicle control (0.1% DMSO) or UCD74A (A) at 250 μ M for 60 min. Glioma cells were exposed to UCD38B at 250 μ M for 15 min or 60 min (B). Co-localization of PAI-1 with late endosomes (LE) using LAMP-1 as a marker protein was visualized in glioma cells treated with vehicle or UCD74A for 60 min (C) or UCD38B (D) for 15 min or 60 min. Scale bar is 50 microns. U87MG glioma cells were imaged and co-localization of immunofluorescent labels quantified using the high content imaging system ImageXpress and analyzed by a custom module using MetaXpress 5.0 software (E). Results are presented as the mean \pm S.D. of $n = 15$ with $***P < 0.001$.

Figure 6. Co-localization of urokinase plasminogen activator (uPA) with early and late endosomes in U87MG glioma cells. Association of uPA with EE using EEA-1 as a marker

protein was analyzed using anti-uPA antibody. U87MG glioma cells were treated for 60 min with either drug vehicle, 250 μ M of UCD74A (**A**) or 250 μ M of UCD38B for 15 min and 60 min (**B**). uPA and LE localization using LAMP-1 as a marker protein was examined in glioma cells treated with drug vehicle (control), UCD74A for 60 min (**C**) or UCD38B for 15 min or 60 min (**D**). Scale bar is 50 microns. Quantification of uPA co-localization with endosomes was determined by imaging U87MG glioma cells using the high content imaging system ImageXpress and analyzed by a custom module using MetaXpress 5.0 software (**E**). Results are presented as the mean \pm S.D. of $n = 15$ with $***P < 0.001$.

Figure 7. Co-localization of urokinase plasminogen activator receptor (uPAR) with early and late endosomes in U87MG glioma cells. Association of uPAR with EE and LE using EEA-1 and LAMP-1 as marker proteins, respectively was analyzed by confocal microscopy. U87MG cells were treated with vehicle control, 250 μ M of UCD74A for 60 min (**A**) and (**C**) or with 250 μ M of UCD3B for 15 min or 60 min (**B**) and (**D**). Scale bar is 50 microns. Quantification of co-localization of uPAR with endosomes was quantified in U87MG glioma cells using the high content imaging system ImageXpress and analyzed with a custom module using MetaXpress 5.0 software (**E**). Results are presented as the mean \pm S.D. of $n = 15$ with $***P < 0.001$.

Figure 8. Co-localization of PAI-1 and LRP-1 in U87MG glioma cells. U87MG cells were treated with either vehicle control, UCD74A or UCD38B at 250 μ M for 60 min. PAI-1 seen in green was immunostained with anti-PAI-1 primary and Alexa 488 secondary antibody. LRP-1 in red is detected by anti-LRP-1 primary and Alexa 594 secondary antibody (**A**). LRP-1 in green was associated with early endosomes immunostained with EEA-1 antibody (red) (**B**).

Colocalization of LRP-1 with late endosomes was detected with LAMP-1 antibody (red) (C).

Scale bar is 50 microns.

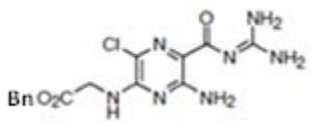
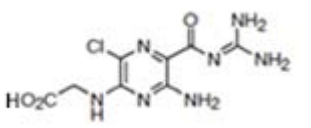
Figure 9. Close proximity of endosomes and mitochondria in UCD38B treated U87MG glioma cells. U87MG cells were treated with either vehicle control, UCD74A or UCD38B at 250 μM for 60 min. Translocation of early and late endosomes was verified by immunocytochemistry, using EEA-1 and LAMP-1, respectively. Mitochondria are visualized in red using MitoTracker. Early endosomes were detected using anti-EEA-1 antibody (A). Late endosomes were detected by anti-LAMP-1 antibody (B). Colocalization of endosomes with mitochondria was quantified using ImagXpress and analyzed with a custom module using MetaXpress 5.0 software. Results are presented as the mean \pm S.D. of $n = 15$ with $***P < 0.001$ (C). U87MG cells were preloaded with JC-1 dye at 5 μM for 15 min and treated with either vehicle control or UCD38B or UCD74A at 250 μM for 75 min. Glioma cells were then fixed for immunocytochemistry to immunostained for late endosomes using anti-LAMP-1 as primary and . Alexa 647 as secondary antibody, respectively (D). Scale bar is 50 microns.

Figure 10. Intracellular UCD38B cytotoxicity. U87MG glioma cells were treated with UCD38B or UCD74A for 2 h at 4 $^{\circ}\text{C}$. The cells were rinsed with PBS and visualized under fluorescent microscope. UCD38B was cell permeant at 4 $^{\circ}\text{C}$ as determined by intracellular fluorescence and UCD74A was cell impermeant. Upper panel shows fluorescence and lower panel shows bright field images at 40X. Scale bar is 50 microns (A). U87MG glioma cells were incubated for 2, 6 and 24 h at 4 $^{\circ}\text{C}$. Glioma cells were washed with 1X PBS, replaced with fresh media with no drug and then transferred to 37 $^{\circ}\text{C}$ for 24 h. Cytotoxicity of intracellular UCD38B was determined by LDH assay (B). PAI-1 co-localization with mitochondria was examined by immunofluorescence. U87MG cells were exposed to UCD38B or UCD74A for 2 h at 4 $^{\circ}\text{C}$

followed by 37 °C shift to induce glioma cell death. Mitochondria and PAI-1 were visualized using MitoTracker and anti-PAI-1 monoclonal antibody, respectively. DAPI was used to stain the nucleus. Scale bar is 50 microns (C).

Figure 11. Proposed model of altered endosomal trafficking following treatment with UCD38B. Cell permeant drug (UCD38B) targets the intracellular uPAS complex relocating the early (1) and the late endosomes (2) to be in close proximity with mitochondrial regions. AIF is released and translocated to the nucleus (3) leading to glioma cell death. We hypothesize that UCD38B disrupts endosomal recycling (4) thereby increasing the intracellular uPA-PAI-1 complex.

Table1. The uPA-PAI-1 complex in glioma cells detected by ELISA

U87MGs treated with drug	uPA-PAI-1 complex in ng/ml
Vehicle, 120 min	4.1 ± 0.03
 UCD38B, 45 min	5.5 ± 0.3**
UCD38B, 120 min	6.2 ± 0.1**
 UCD74A, 120 min	4.1 ± 0.06

uPA-PAI-1 complex was determined by ELISA following drug treatment. U87MG glioma cells were treated with UCD38B for 45 min and 2 h or with UCD74A for 2 h. Protein extracts were made and 0.5mg/ml of total protein was used for detection of the uPA-PAI-1 complex. Results are presented as the mean ± S.D. of $n = 3$. * Significant $P < 0.05$, ** $P < 0.01$

Figure 1

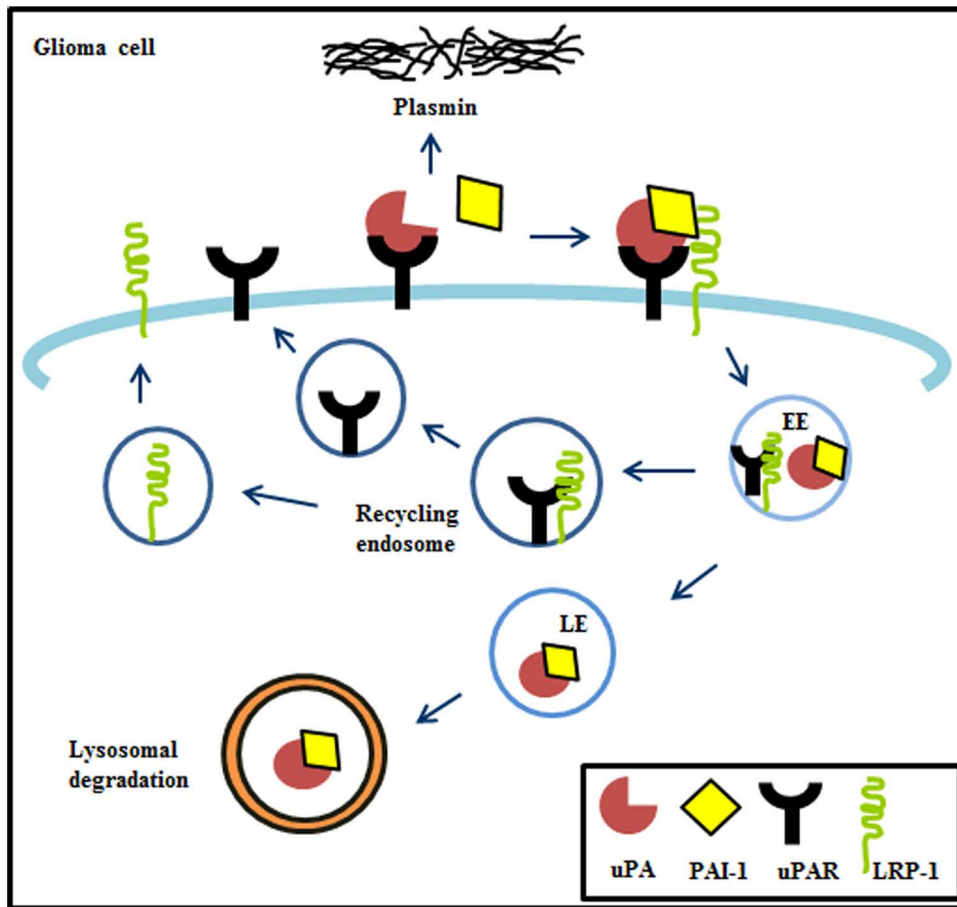
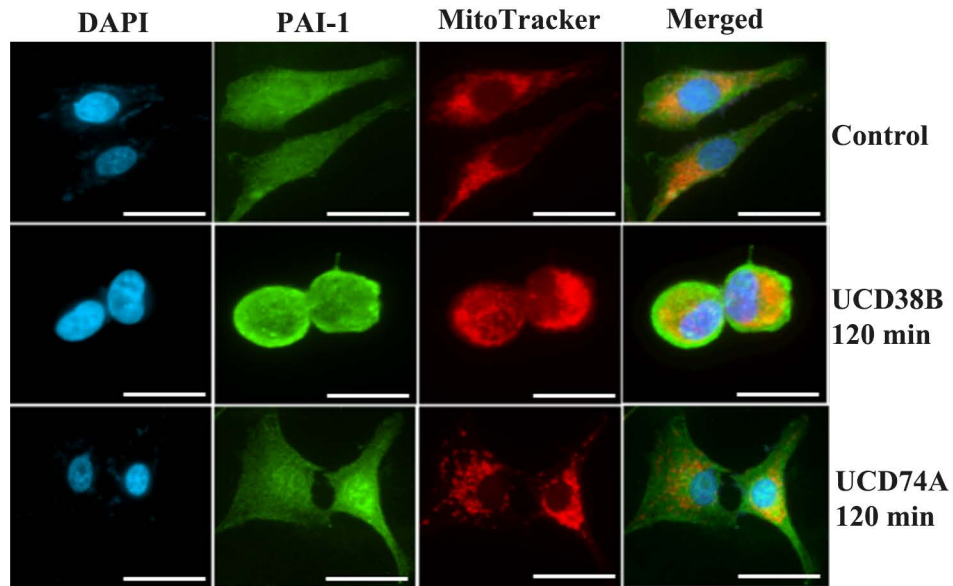
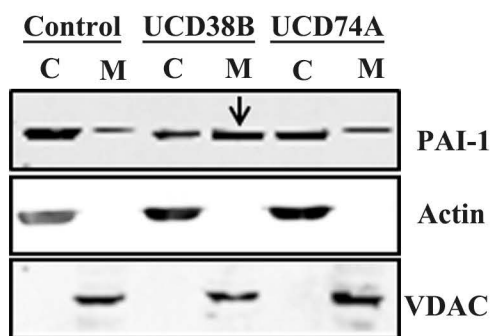


Figure 2

A



B



C

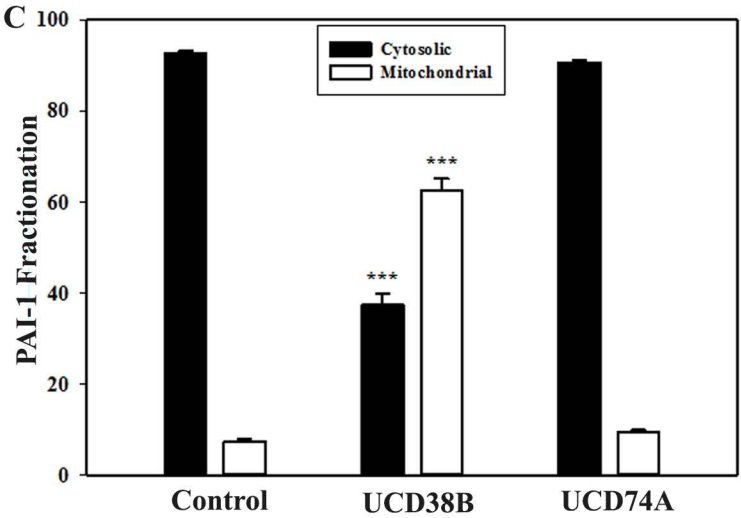
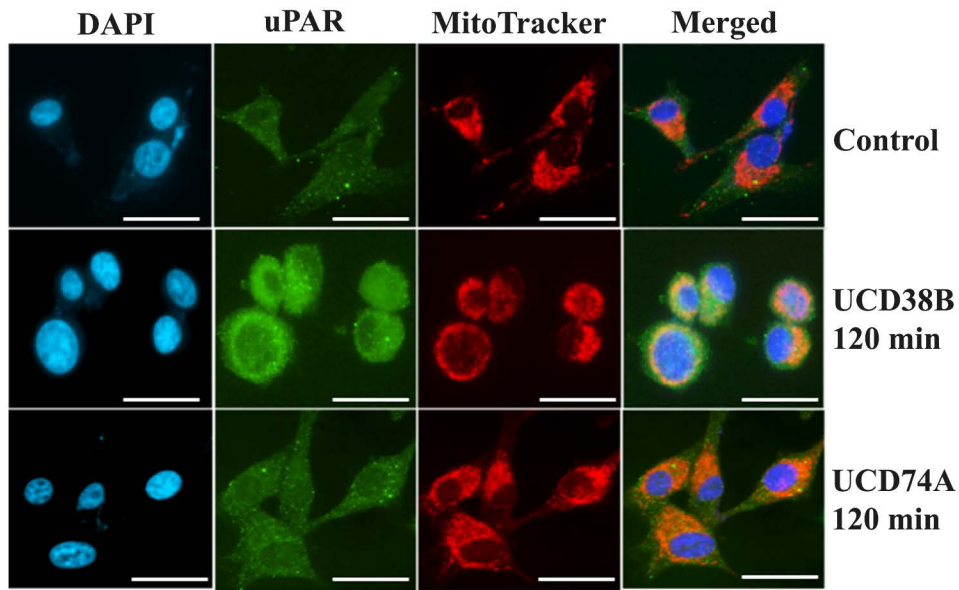


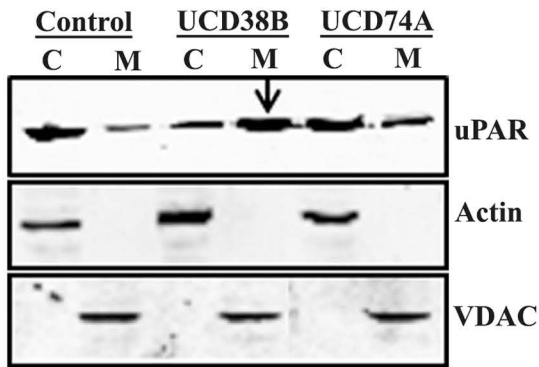
Figure 3

Molecular Pharmacology Fast Forward. Published on January 29, 2015 as DOI: 10.1124/mol.114.096602
This article has not been copyedited and formatted. The final version may differ from this version.

A



B



C

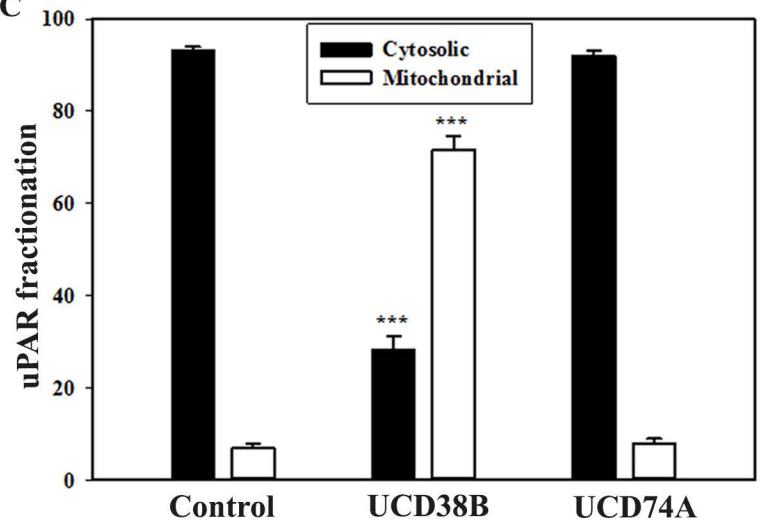


Figure 4

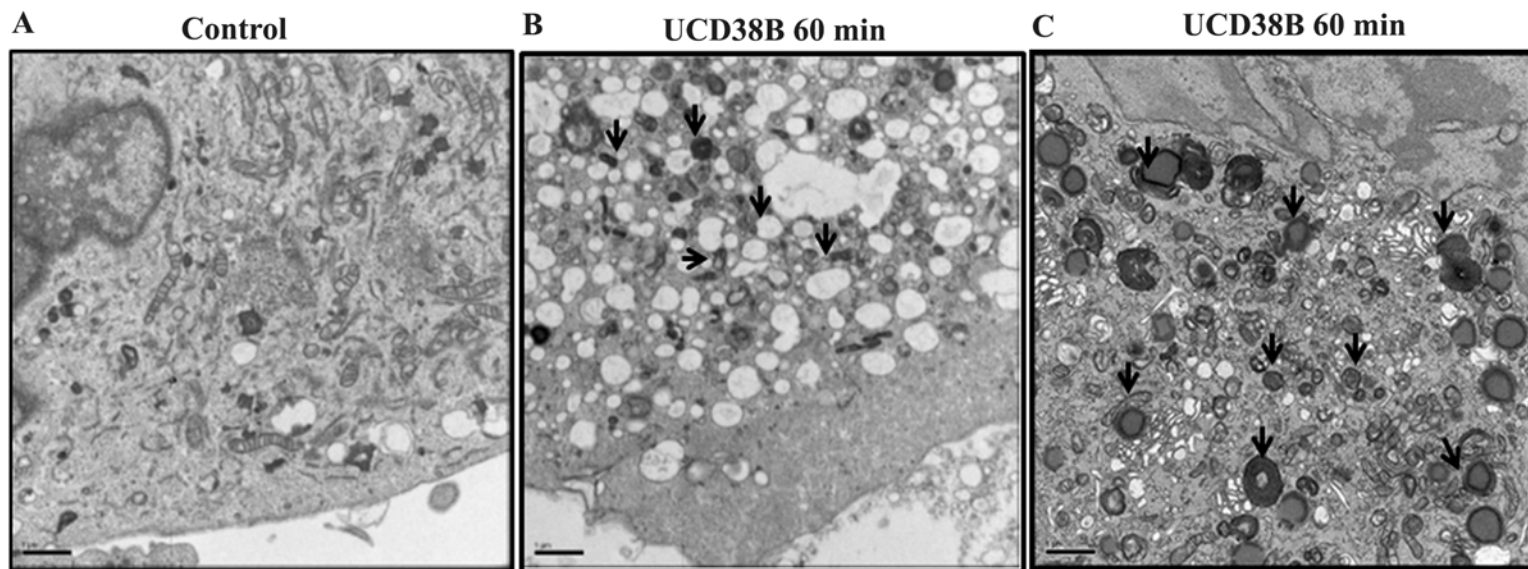


Figure 3

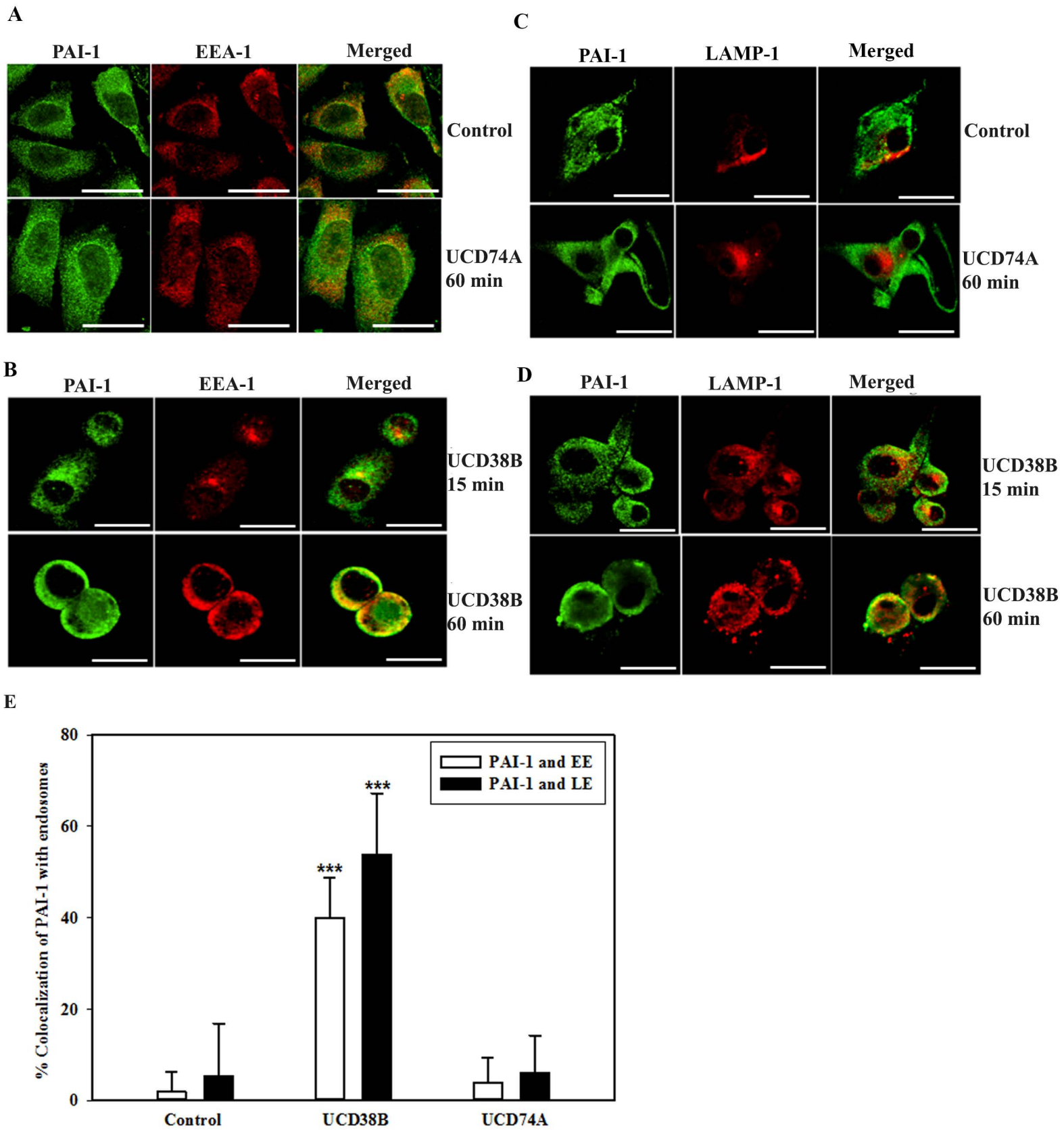


Figure 6

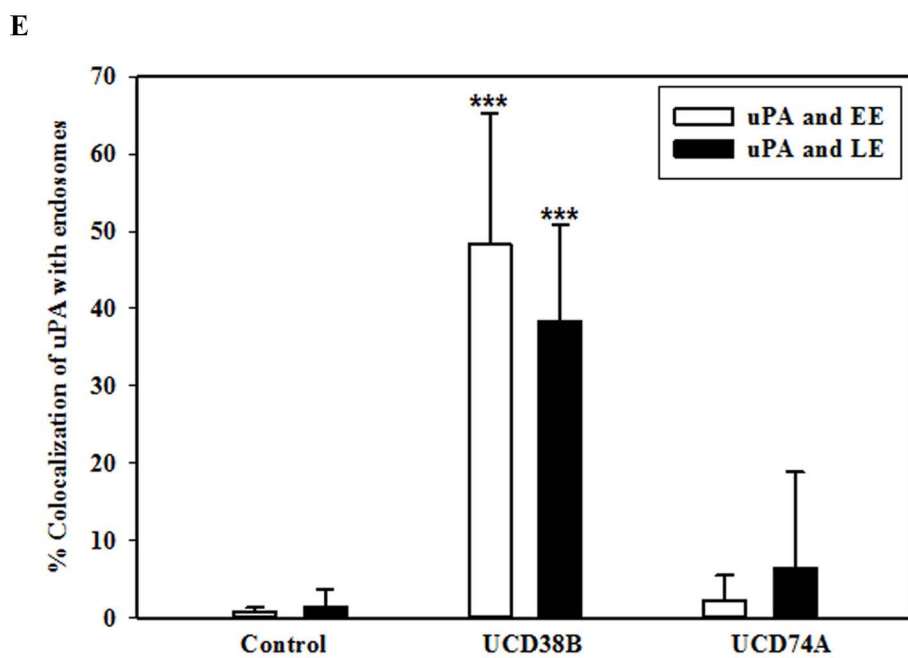
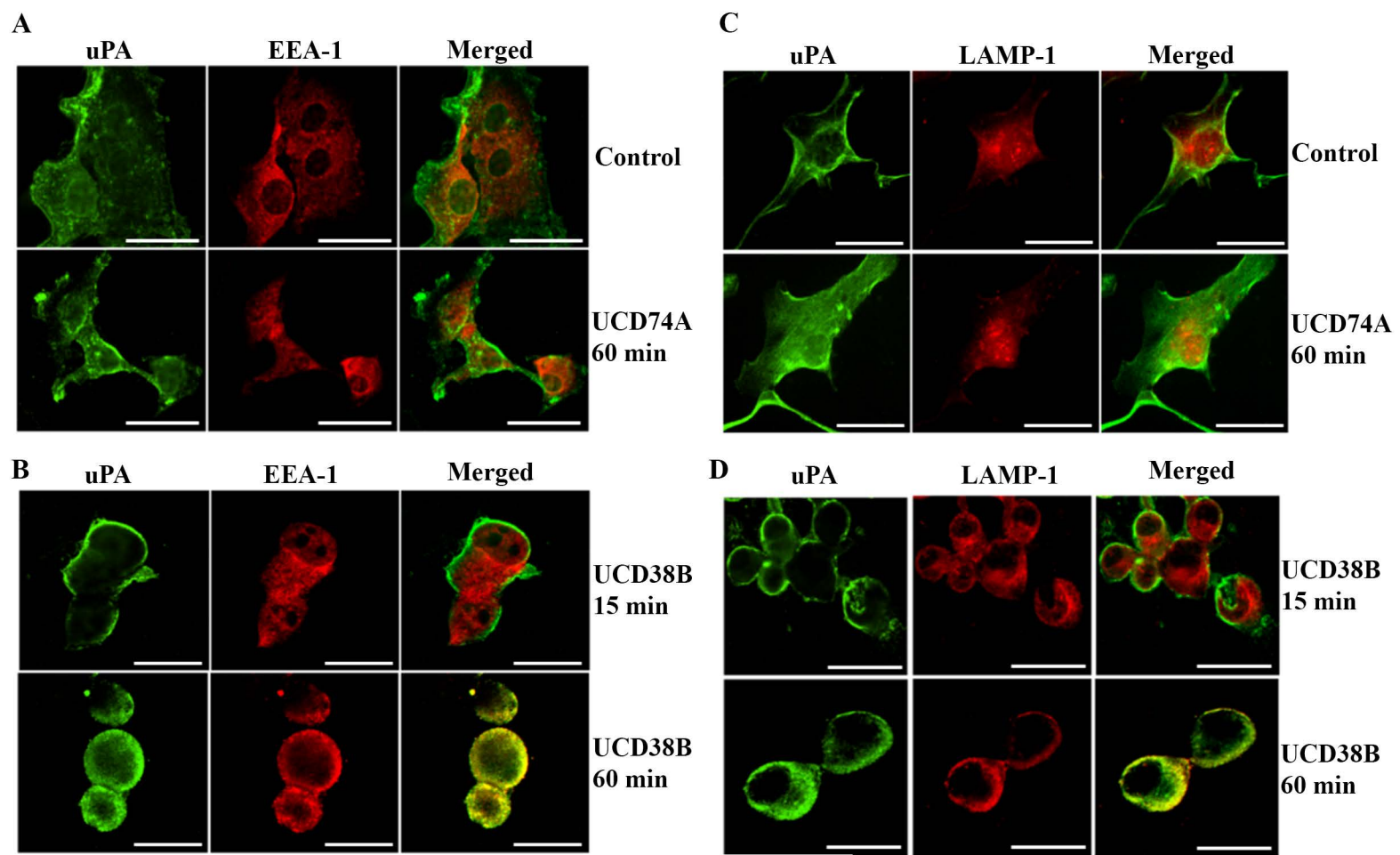


Figure 7

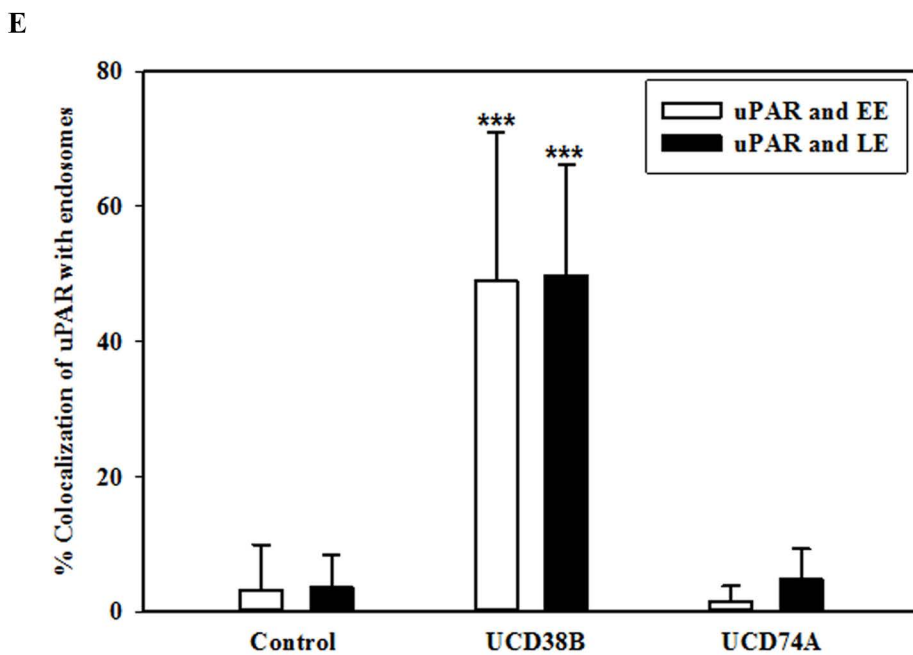
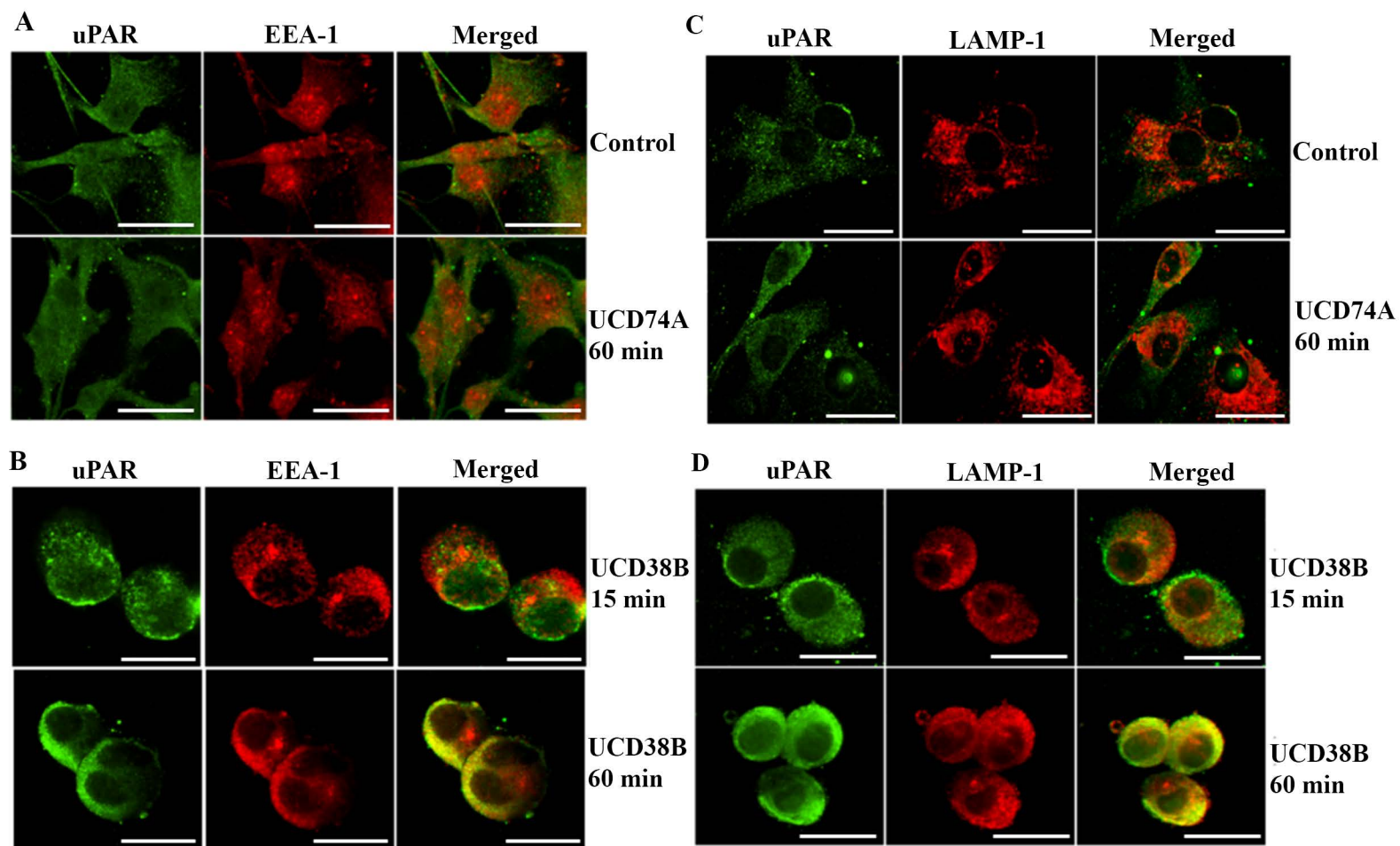


Figure 8

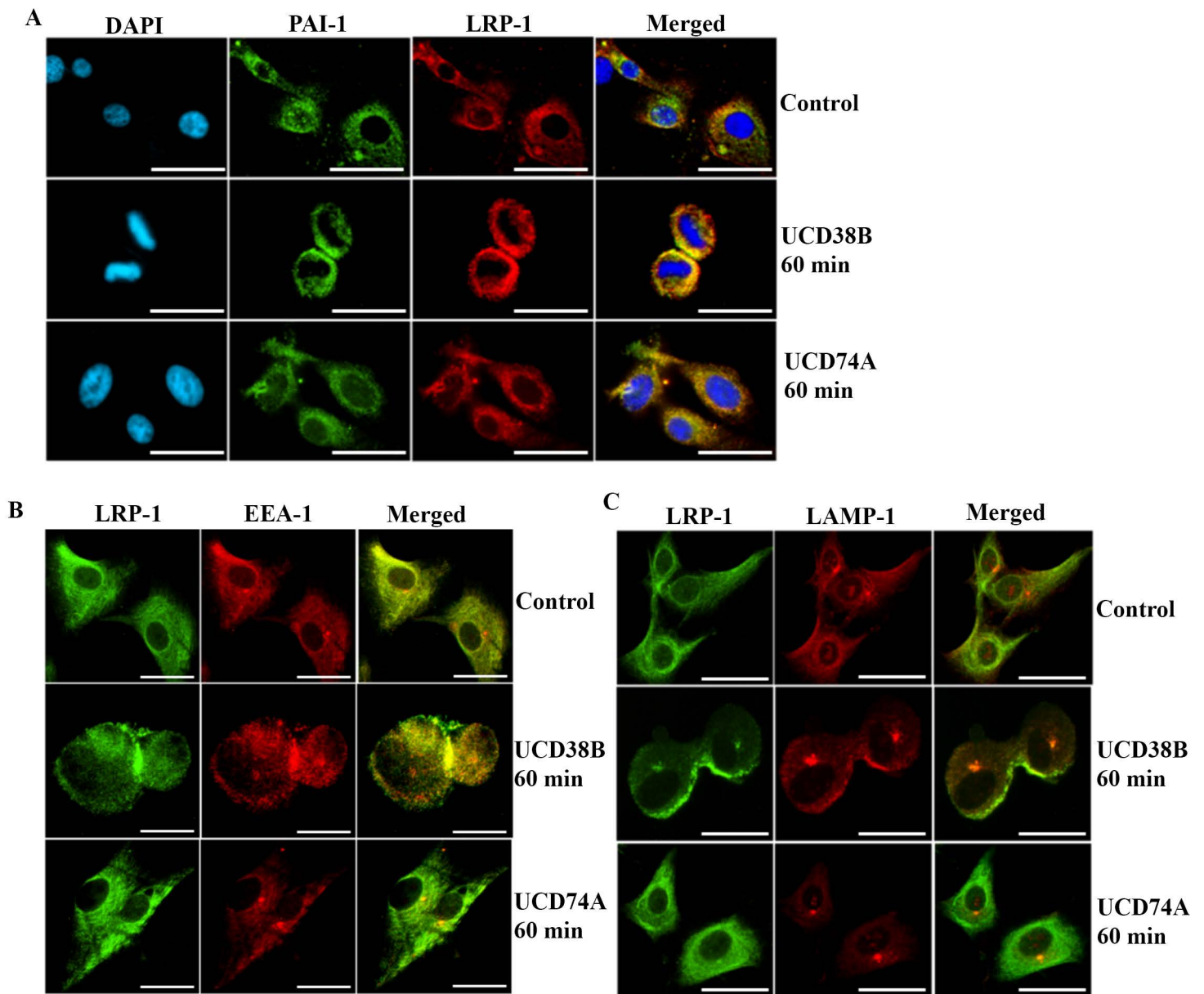


Figure 9

Molecular Pharmacology Fast Forward. Published on January 29, 2015 as DOI: 10.1124/mol.114.096602
 Mitochondria has not been certified and formatted. The final version may differ from this version.

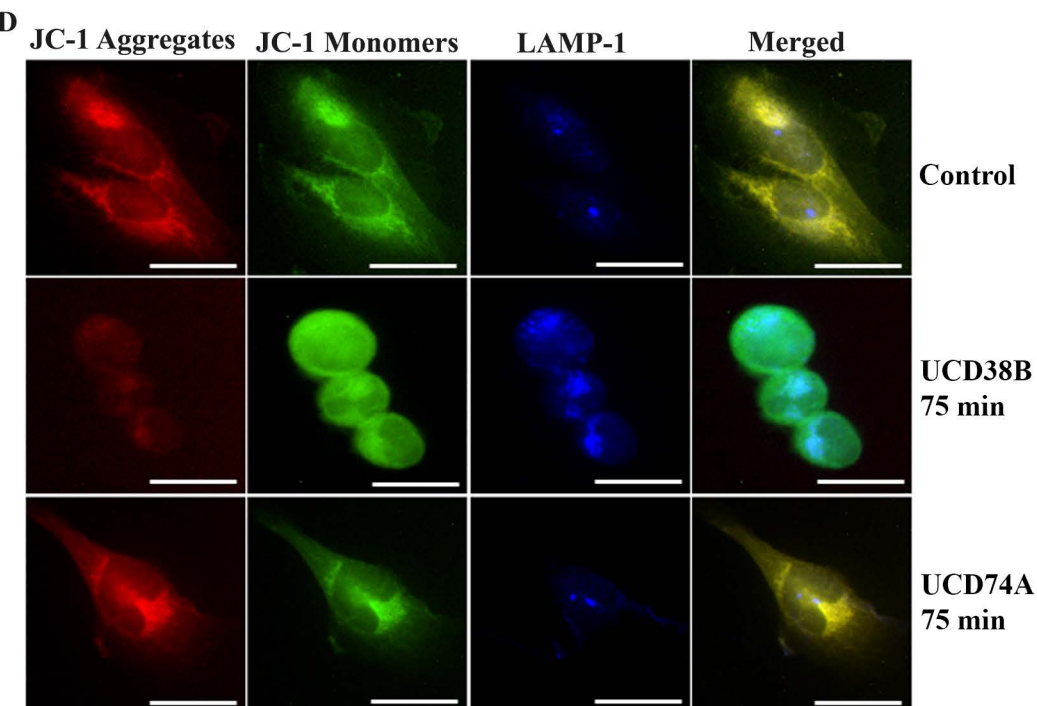
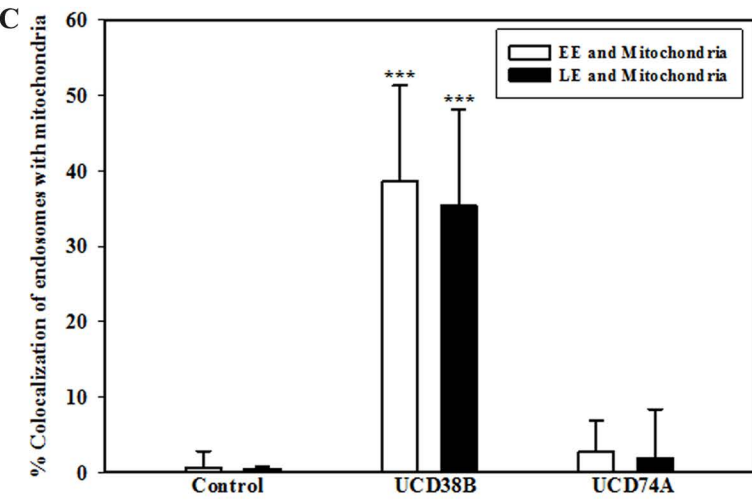
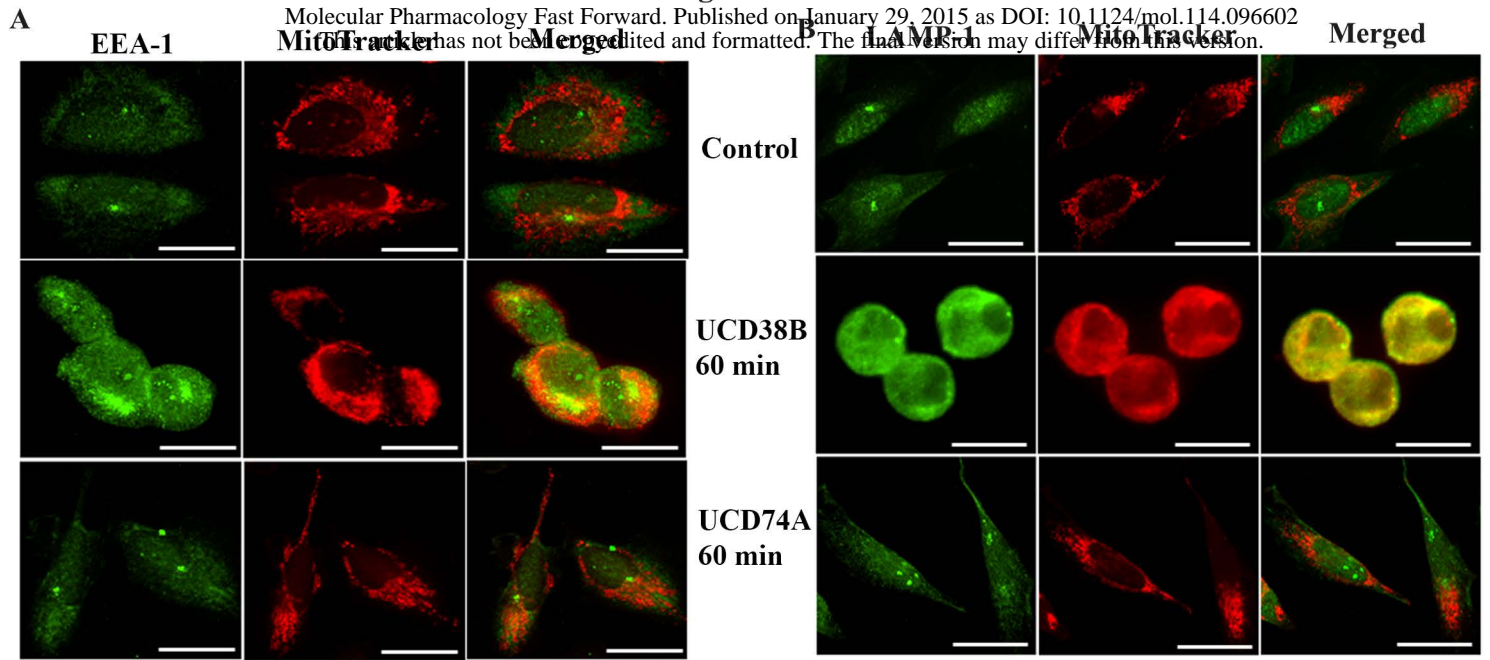
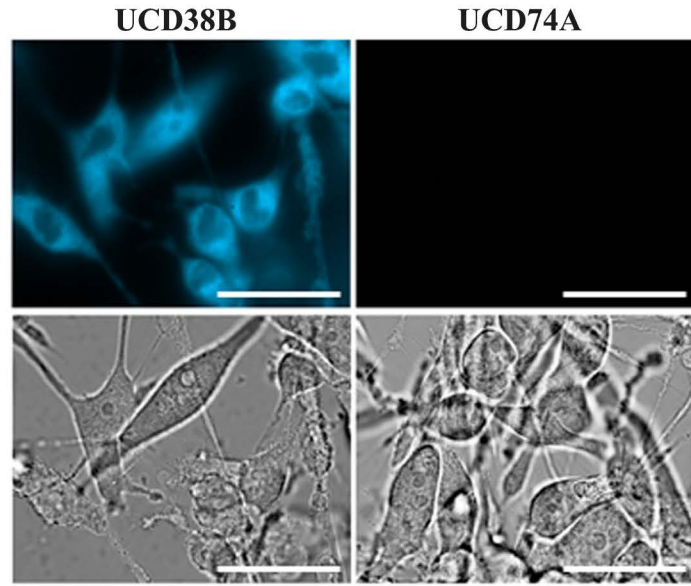


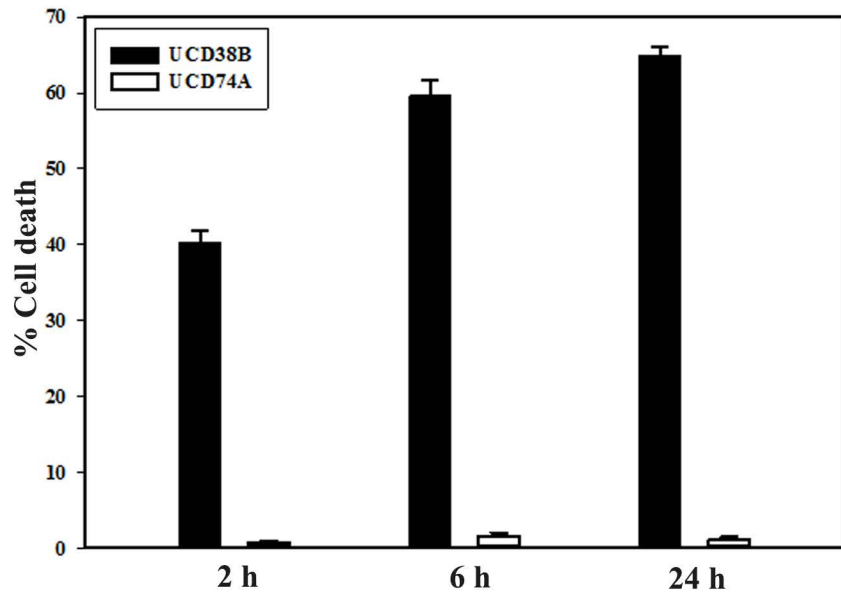
Figure 10

Molecular Pharmacology Fast Forward. Published on January 29, 2015 as DOI: 10.1124/mol.114.096602
This article has not been copyedited and formatted. The final version may differ from this version.

A



B



C

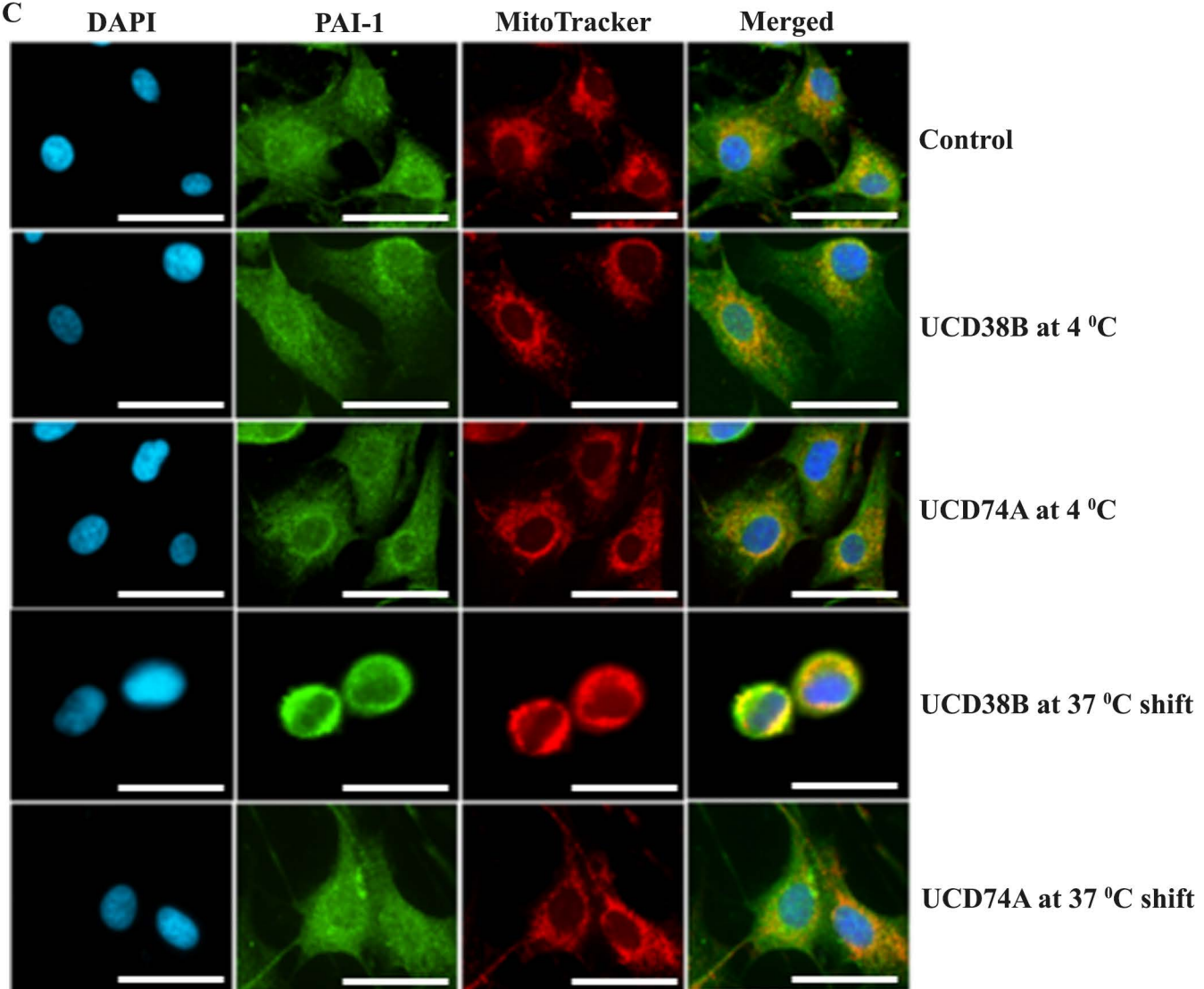


Figure 11

